



Article

FAST Low-Energy Beamline Studies: Toward High Peak 5-D Brightness Beams for FAST-GREENS

F. Cropp^{1*}, J. Ruan², J. Santucci², D. MacLean², A. Lumpkin², C. Hall³, J. Edelen³, A. Murokh⁴, D. Broemmelsiek² and P. Musumeci¹

¹ Department of Physics and Astronomy, University of California, Los Angeles, Los Angeles, California 90095, USA

² Fermi National Accelerator Laboratory, Batavia, Illinois 60510, USA

³ RadiaSoft, Boulder, CO 80301, USA

⁴ RadiaBeam Technologies, Santa Monica, CA 90404, USA

* Correspondence: ericcropp@physics.ucla.edu

Abstract: The FAST beamline is the injector for the planned Gamma-Ray Electron ENhanced Source (GREENS) program, which aims at demonstration and first application of a high efficiency high average power free-electron laser at 515 nm. FAST-GREENS requires high 5-D peak brightness; transverse normalized projected emittances of 3 mm-mrad and a peak current of 600 A are the minimum beam requirements for the FEL to reach the 10 % efficiency goal. In this work, studies of the low-energy section of the FAST beamline are presented toward these ends, including preliminary measurements of beam compression and beam emittance. An effort toward developing a high-fidelity simulation model that could be later optimized for FAST-GREENS is presented.

Keywords: High Brightness Beams; Accelerator Modeling; Particle Tracking Simulation

1. Introduction

The Fermilab Accelerator Science and Technology (FAST) facility is host to several current and proposed projects of notable scientific merit. These include Integrable Optics Test Accelerator (IOTA) [1], the under-construction FAST Gamma-Ray Electron Enhanced Source (GREENS) [2], and upcoming photocathode studies in a high-gradient photoinjector proposed by the Center for Bright Beams.

For FAST-GREENS, the requirements on peak 5-D beam brightness from the injector are particularly demanding. To these ends, FAST-GREENS will require the FAST injector to run near the boundary of capability on the Pareto front of beam charge vs. transverse emittance. Indeed, the nominal requirements of 3-mm-mrad emittance in each dimension, along with a peak current of 600 A will require careful optimization of the upstream injector parameters on an offline model.

This article reports on the development of a high-fidelity model of FAST for optimization toward high peak 5-D beam brightness for FAST-GREENS. Additionally, proposed work to deduce photocathode properties from solenoid scans at FAST will benefit greatly from such a model, as such studies require a model to invert/optimize (e.g. [3]).

2. Materials and Methods

The FAST beam line (shown in Fig. 1) starts with the gun, of similar type to the DESY-PITZ gun [4]. The 1.3-GHz, 1.5-cell cavity is followed by an emittance compensation solenoid, with adjustable position. The bucking solenoid directly upstream of the gun is generally set to produce a magnetic field in the opposite direction of the main solenoid at a magnitude such that the field at the photocathode is zero, so that the beam is born with zero angular momentum. The gun has an INFN-style load lock system that allows for the exchange of photocathodes. Two TESLA cavities [5] (CC1 & CC2 in Fig. 1 are used to

Citation: Cropp, F.; Ruan, J.; Santucci, J.; MacLean, D.; Lumpkin, A.; Hall, C.; Edelen, J.; Murokh, A.; Broemmelsiek, D.; Musumeci, P. FAST Low Energy Beamline Studies: Toward High Peak 5-D Brightness Beams for FAST-GREENS. *Instruments* **2023**, *1*, 0. <https://doi.org/>

Received:

Revised:

Accepted:

Published:

Copyright: © 2023 by the authors. Submitted to *Instruments* for possible open access publication under the terms and conditions of the Creative Commons Attribution (CC BY) license (<https://creativecommons.org/licenses/by/4.0/>).

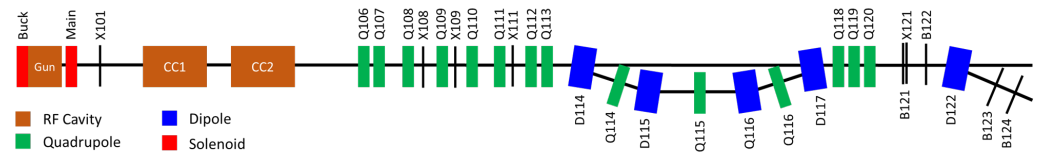


Figure 1. The FAST injector, with selected diagnostics shown. Q106, Q107 and Q111 are 45 degree skew quadrupoles. Diagnostics with X delineation are screens (YAG or OTR), while those delineated with a B are noninvasive beam position monitors (BPM).

accelerate the beam to 35-50 MeV in nominal cases. A series of quadrupoles are used to manipulate the beam transversely. The quadrupoles are followed by a chicane that is used to compress the beam. The chicane can also be bypassed and the beam can be directed from Q113 to Q118, the start of a quadrupole triplet. Following B122, the beam energy can be measured on the beam dump line.

As mentioned above, one of the primary goals of this study is to provide a model for optimization of compression in the chicane. In a chicane, beam emittance will be diluted by coherent synchrotron radiation (CSR) effects, which must be modeled properly. To these ends, General Particle Tracer (GPT) [6] has been shown to be a good choice to model 3D CSR effects [7]. As such, GPT was chosen as the physics model to use in this effort.

There are numerous free parameters for the model. Table 1 lists the free parameters and the data taken to fit them.

Table 1. Free parameters in the model and the tests completed to fit these parameters .

Parameter	Data
Main Solenoid Position	Main Solenoid Scan & Downstream Images
Bucking Solenoid Position	Bucking Solenoid Scan
X101 Position	Main Solenoid Scan & Downstream Images
Gun Peak Field	CC1 Energy Scan
Gun Phase	Gun Phase Scan
Initial Pulse Length	Gun Phase Scan & Streak Camera Images
Beam Initial Transverse Size	Virtual Cathode Image
Solenoid Strengths	Solenoid Magnetic Measurements
CC1 Peak Field	CC1 Energy Scan & Downstream Images
CC1 Phase	CC1 Energy Scan

3. Results

3.1. Longitudinal Dynamics

In order to verify the longitudinal dynamics of the beam and match a model, two tests were performed: a gun phase scan and a streak camera measurement at X121 (see Fig. 1), approximately 17.4 m downstream of the photocathode. Both will be described below.

For the first test, the gun phase was changed in 0.2 degree intervals and extracted charge was measured at the exit of the gun. The time it takes for the beam to be extracted from the cathode can be measured from this scan. Neglecting the Schottky effect, under purely classical conditions, where the laser induces above threshold photoemission, the measured charge should start as soon as the RF phase is such that the field accelerates the head of the bunch downstream. As the phase is increased, more of the bunch experiences an accelerating field, until the full bunch does, at which point the full beam charge is measured. Based on the degrees of phase sampled between first electrons and full beam, the length of the pulse from the gun can be determined. For a uniform distribution, the rise would be linear, but for a Gaussian beam, the rise can be modeled as an error function.

However, this is a simplified picture. In fact, as the RF phase changes, the magnitude of the field at the cathode also changes, which changes the tunneling probability of the electrons. As such, we have to take into account the Schottky enhancement on the quantum efficiency:

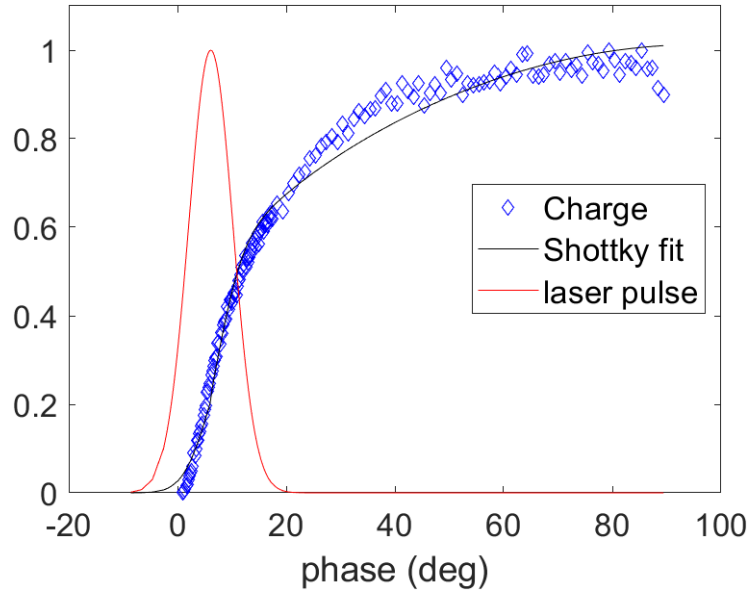


Figure 2. RMS laser pulse length fit with a Schottky fit.

$$QE \propto (E_{excess})^2 \quad (1)$$

where

$$E_{excess} = h\nu - \phi_w + \phi_{Schottky} \quad (2)$$

and

$$\phi_{Schottky} = \sqrt{\frac{e}{4\pi\epsilon_0}} \sqrt{\beta E_0 \sin(\theta)} \quad (3)$$

where $h\nu$ is the photon energy and ϕ_w is the nominal work function of the photocathode. E_0 is the magnitude of the electric field, while θ is the RF phase. In practice, the constants, $\sqrt{\frac{e}{4\pi\epsilon_0}}$ can be lumped into β , the Schottky enhancement factor, in a fit. As such, the error function can be combined with the Schottky fit to fit the initial pulse length. At FAST, this yielded an 8.6ps RMS initial pulse length, as shown in Fig. 2.

The electron beam bunch length was also measured after the compressor using a streak camera setup at X121. This measurement used an OTR screen and used the streak camera method established in numerous studies (e.g. in [8]) to characterize the pulse length. These yielded comparable results to the GPT simulations, when factoring in a resolution term due to the height of the collimating slit width for the streak camera measurement. See Fig. 3 for details.

The beam energy was measured using a dipole spectrometer. Using the geometry of the system and the magnetic field in D122 (as shown in the Fig. 1), the beam kinetic energy can be calculated using the relationship $B\rho = pc/e$ where B is the magnetic field, ρ is the bending radius of the magnet and p is the beam momentum. ρ is determined by the geometry of the system. By varying the phase in CC1, the beam energy can be controlled directly. Given that the a sinusoidal energy kick imparted by CC1, the kinetic energy of the gun can also be deduced.

$$E_{kin} = E_{gun} + E_{CC1} \cos(\theta) \quad (4)$$

The geometry of the system is determined by four non-destructive BPMs, B121, B122, B123, and B124 in Fig. 1. The latter two of these BPMs are in the dogleg beamline. As such, both the beam position and angle of the beam can be determined before and after

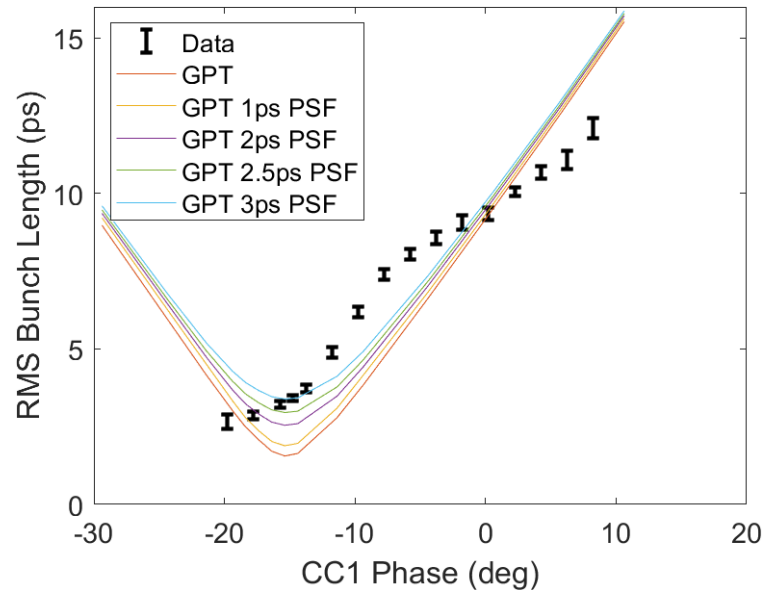


Figure 3. Measured compression using CC1 and the chicane for compression. Streak camera measurements are overlaid with GPT predictions convolved with a resolution term (PSF).

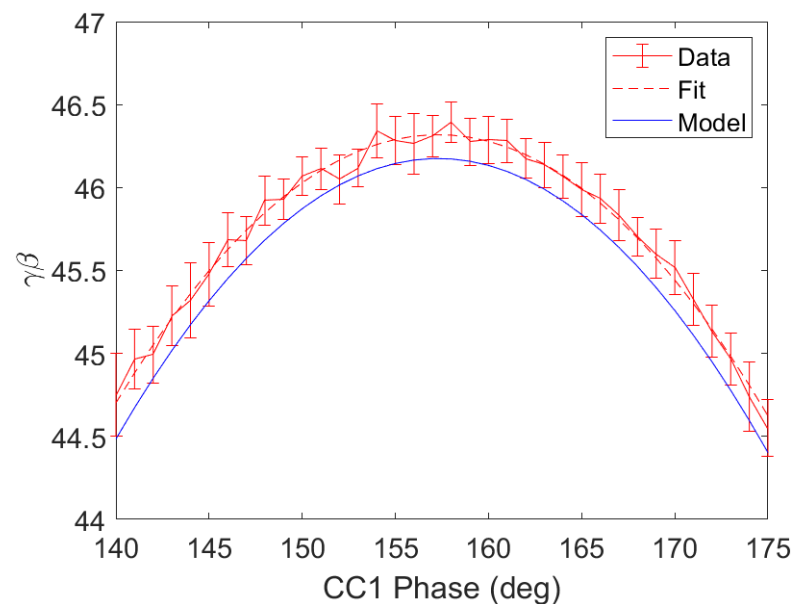


Figure 4. Kinetic energy measurements as a function of CC1 phase.

the dipole. While the probe inside the dipole gives a readback on the magnetic field inside the dipole, this measurement has systematic (mostly due to calibration errors and physical misalignment) and measured error associated with it. As such, the energy in the preliminary GPT model is adjusted slightly to match the transverse behavior described below. See Fig. 4.

3.2. Transverse Dynamics

On the transverse side, a virtual cathode camera image was recorded on each run day. This was used to start a distribution of particles in simulation.

Solenoid scans were measured on screen X101. The position of the screen is considered to be a free parameter within a range of the estimated position of 1.062 meters downstream of the photocathode. See Fig. 5 for more details. The best fit puts the screen approximately 5 cm upstream in simulation relative to the center of this range. Note that in simulation,

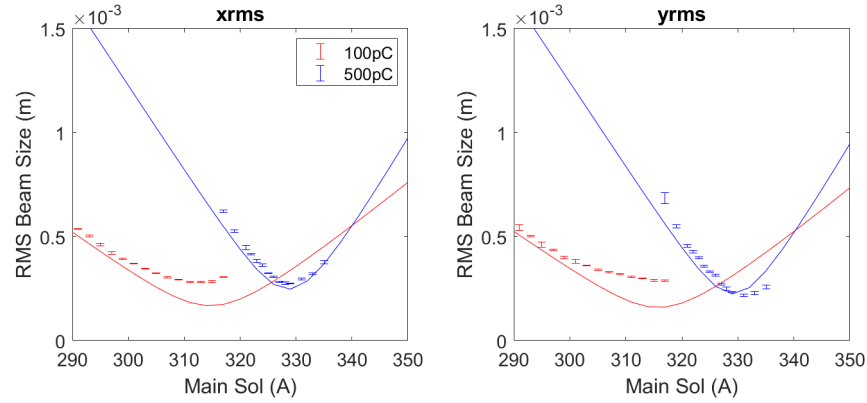


Figure 5. Example solenoid scans at multiple charges with GPT predictions overlaid.

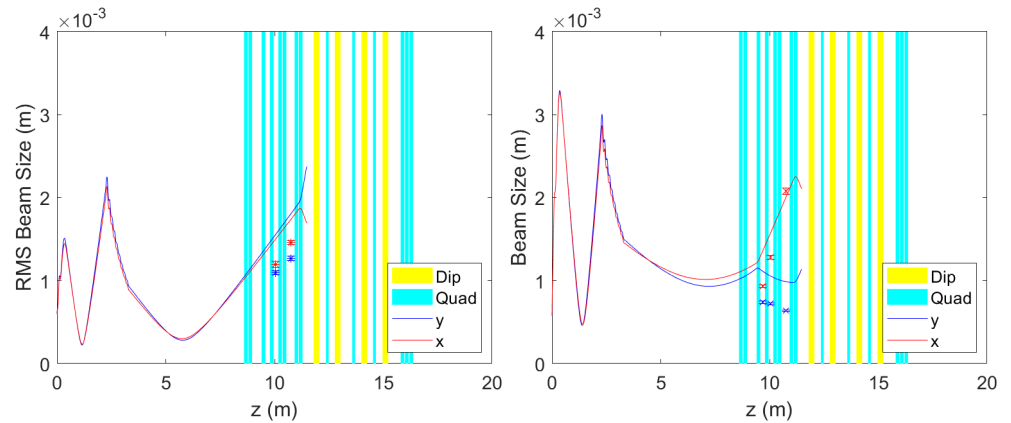


Figure 6. Downstream beam second order moments indicated with markers, shown with GPT predictions for an approximately 100pC beam (left) and an approximately 700pC beam (right).

the positions of the solenoids have been also kept as free parameters, as these magnets can be translated along the beamline. The main solenoid was positioned 32 cm downstream of the photocathode.

Importantly, the transverse beam sizes were measured at X108 (when available), X109 and X111 and compared to simulation for various charges. See qualitative agreement with preliminary model in Fig. 6.

The transverse emittance was measured using the two quadrupole scan method [9]. Generally, the retrieved emittance is higher than predicted by the preliminary model. For example, the projected emittance of an approximately 700pC beam was approximately 20 mm mrad in each dimension with skew quadrupoles on, while the simulated RMS normalized projected emittance was approximately 9 mm mrad in x and 17 mm mrad in y .

4. Discussion

Preliminary measurements of the photoinjector beam dynamics and comparison with a newly developed GPT model of FAST are presented. While the simulations qualitatively match the behavior observed in experiment, there are still significant discrepancies that will need to be improved before quantitatively relying on the beam quality predictions from the model.

There is a clear asymmetry between x and y beam sizes in the solenoid scans. Some of it can be attributed to the elliptical shape of the laser on the photocathode (which is included in the simulation). But it is very likely that skew and normal quadrupole component in the solenoids or RF fields additionally contributed to the development of this asymmetry. These spurious quadrupole moments could be introduced in the model, but without a direct measurements of the fields (which should be avoided as it would shut down the facility for a long time), the best option is to acquire a complete set of data for varying laser

spot sizes and solenoid values to characterize the injector. This asymmetry could be one of the main reasons for a larger emittance value in the experiment than in simulation. Other possible reasons for the discrepancy include non uniformities in the beam distribution at the cathode (both transverse and longitudinal) giving rise to non linear space charge or stronger CSR effects.

In order to reach the best possible beam quality needed for the high efficiency FEL it will be important for the second RF cavity CC2 to be online as this will allow to compress the beam at higher energy and preserve better the cathode emittance. Finally, the transport in the cryomodule and up to the undulator will need to be simulated and benchmarked with experiments as well.

Author Contributions: Conceptualization, P.M., D.B. and A.M.; methodology, F.C. and P.M.; analysis, F.C.; software, F.C., C.H., J.E., data acquisition, J.R., J.S., D.M. and A.L.; writing—original draft preparation, F.C.; writing—review and editing, F.C. and P.M.; supervision, P.M. and D.B. All authors have read and agreed to the published version of the manuscript.

Funding: This work was supported by the NSF under Grant No. PHY-1549132 and contract number DE-AC02-07CH11359 with the US Department of Energy Office of Science, Office of High Energy Physics.

Conflicts of Interest: The authors declare no conflict of interest.

References

1. Antipov, S.; Broemmelsiek, D.; Bruhwiler, D.; Edstrom, D.; Harms, E.; Lebedev, V.; Leibfritz, J.; Nagaitsev, S.; Park, C.; Piekartz, H.; et al. IOTA (Integrable Optics Test Accelerator): facility and experimental beam physics program. *Journal of Instrumentation* **2017**, *12*, T03002. <https://doi.org/10.1088/1748-0221/12/03/T03002>.
2. Musumeci, P.; Agustsson, R.; Amoudry, L.; Broemmelsiek, D.; Bruhwiler, D.; Denham, P.; Edelen, J.; Fisher, A.; Hall, C.; Hodgetts, T.; et al. FAST-GREENS: A High Efficiency Free Electron Laser Driven by Superconducting RF Accelerator. In Proceedings of the 13th International Particle Accelerator Conference (IPAC'22), Bangkok, Thailand, 12-17 June 2022. JACOW Publishing, Geneva, Switzerland, 2022.
3. Bazarov, I.; Cultrera, L.; Bartnik, A.; Dunham, B.; Karkare, S.; Li, Y.; Liu, X.; Maxson, J.; Roussel, W. Thermal emittance measurements of a cesium potassium antimonide photocathode. *Applied Physics Letters* **2011**, *98*, 224101, [https://pubs.aip.org/aip/apl/article-pdf/doi/10.1063/1.3596450/13353170/224101_1_online.pdf]. <https://doi.org/10.1063/1.3596450>.
4. Stephan, F.; Boulware, C.H.; Krasilnikov, M.; Bähr, J.; Asova, G.; Donat, A.; Gensch, U.; Grabosch, H.J.; Hänel, M.; Hakobyan, L.; et al. Detailed characterization of electron sources yielding first demonstration of European X-ray Free-Electron Laser beam quality. *Phys. Rev. ST Accel. Beams* **2010**, *13*, 020704. <https://doi.org/10.1103/PhysRevSTAB.13.020704>.
5. Aune, B.; Bandelmann, R.; Bloess, D.; Bonin, B.; Bosotti, A.; Champion, M.; Crawford, C.; Deppe, G.; Dwersteg, B.; Edwards, D.A.; et al. Superconducting TESLA cavities. *Phys. Rev. ST Accel. Beams* **2000**, *3*, 092001. <https://doi.org/10.1103/PhysRevSTAB.3.092001>.
6. General Particle Tracer. <http://www.pulsar.nl/gpt/>.
7. van der Geer, S.; Brynes, A.; Setija, I.; Smorenburg, P.; Williams, P.; de Loos, M. GPT-CSR: a New Simulation Code for CSR Effects. In Proceedings of the Proc. 9th International Particle Accelerator Conference (IPAC'18), Vancouver, BC, Canada, April 29-May 4, 2018, Geneva, Switzerland, June 2018; Number 9 in International Particle Accelerator Conference, pp. 3414–3417. <https://doi.org/10.18429/JACoW-IPAC2018-THPAK078>, <https://doi.org/doi:10.18429/JACoW-IPAC2018-THPAK078>.
8. Lumpkin, A.; Thurman-Keup, R.; Edstrom Jr, D.; Ruan, J.; Santucci, J. Initial observations of micropulse elongation of electron beams in a SCRF accelerator. *arXiv preprint arXiv:1712.09616* **2017**.
9. Prat, E.; Aiba, M. Four-dimensional transverse beam matrix measurement using the multiple-quadrupole scan technique. *Physical Review Special Topics-Accelerators and Beams* **2014**, *17*, 052801.

Disclaimer/Publisher's Note: The statements, opinions and data contained in all publications are solely those of the individual author(s) and contributor(s) and not of MDPI and/or the editor(s). MDPI and/or the editor(s) disclaim responsibility for any injury to people or property resulting from any ideas, methods, instructions or products referred to in the content.